Available online at www.sciencedirect.com
SCIENCE DIRECT®
PERGAMON
Acta Astronautica 52 (2003) 619–628
ACTA ASTRONAUTICA
www.elsevier.com/locate/actaastro

Analysis and testing of similarity and scale effects in hybrid rocket motors

Rajeshwar Dayal Swami, Alon Gany*

Faculty of Aerospace Engineering, Technion-Israel Institute of Technology, Haifa 32000, Israel

Received 29 January 2001; received in revised form 22 November 2001

Abstract

In order to derive proper scaling rules in hybrid rocket motors, a theoretical similarity analysis is presented. By taking account of the main phenomena and effects, the similarity analysis defines the following three main conditions for testing a laboratory-scale hybrid rocket motor that can simulate a full-scale motor: (1) geometric similarity, (2) same fuel and oxidizer combination, and (3) scaling mass flow rate of oxidizer in proportion to the motor port diameter. To verify the analysis, tests are conducted on different-size polymethylmethacrylate/gaseous oxygen hybrid rocket motors. These motors are scaled as per the similarity analysis and tested under similarity conditions. A fairly good agreement between the test-results and theoretical prediction verifies the similarity model. This also points out that the main processes and effects associated with hybrid rocket combustion have been considered adequately in the analysis.

1. Introduction

The hybrid rocket motor has attracted a renewed attention for propulsion system application because of its distinct advantages such as simplicity, safety, good performance, comparatively cleaner environmental characteristics, and lower cost, particularly compared to solid propellant rockets. In a typical arrangement, a hybrid rocket motor comprises of a cylindrical polymeric solid fuel grain having a single- or multi-port shape, placed in the combustor and burned with an oxidizer flowing through its ports. As a result, a gas phase diffusion flame is established between the fuel gasification products and the oxidizer within the port flow boundary layer developing over the condensed fuel surface. A typical, single-port hybrid rocket motor geometry with its main combustion and flow characteristics is illustrated in Fig. 1.

The fundamental phenomena associated with hybrid rocket combustion were studied by many investigators [1–3] and reviewed in textbooks [4,5]. These studies revealed the complicated combustion process typical of a hybrid rocket motor, which is characterized by complex interaction among numerous physical phenomena simultaneously occurring in the motor. Nevertheless, owing to its complexity, the prediction of hybrid motor characteristics has generally been based on simplified empirical methods and correlations. Such correlations involve various numerical parameters and constants in order to suitably fit the observed trends. Consequently, actual aspects concerning hybrid rocket combustion are masked. As a result, prediction based on these correlations when applied to different-scale and operating parameters often leads to erroneous results. The study by Estey

* Corresponding author.
E-mail address: gany@tx.technion.ac.il (A. Gany).

0094-5765/02/$ - see front matter
PII: S0094-5765(02)00126-1

Nomenclature

A	area
a	speed of sound
c^*	characteristic velocity
c_p	specific heat at constant pressure
d	diameter
F	thrust
G	mass flux
g	standard gravity acceleration
h	heat transfer coefficient
I_{sp}	specific impulse
L	fuel grain length
L_v	heat of vaporization or gasification
M	mach number
$\dot{m}$	mass flow rate
Nu	nusselt number
n	mass flux exponent in regression rate equation
O/F	oxidizer to fuel (mass) ratio
Pr	prandtl number
p	pressure
$\dot{q}$	heat transfer rate
R	gas constant
Re	Reynolds number
$\dot{r}$	regression rate
T	temperature
t	time
u	axial velocity
γ	specific heat ratio (c_p/c_v)
η	combustion efficiency
λ	heat conduction coefficient
μ	viscosity
ρ	density
τ	characteristic time

Subscripts

a	ambient conditions
b	burning
c	average properties at the end of combustor
ch	chemical
e	nozzle exit
f	flame; fuel
i	initial
ig	ignition
ox	oxygen
p	port
res	residence
s	solid
w	wall

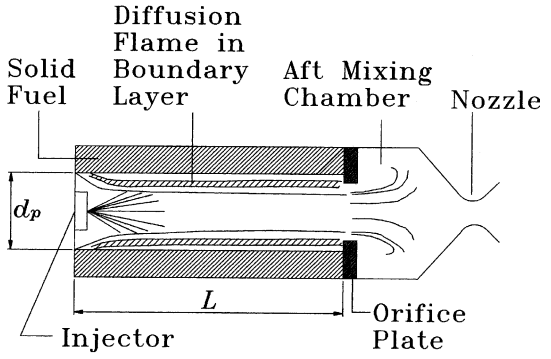

Fig. 1. Representative geometry of a hybrid rocket motor.

et al. [6], although includes useful data and discussions, emphasizes the limitations of such parametric correlations aimed at extrapolation to different scales.

In order to define relevant scaling rules in the field of combustion, many investigators have used the concept of theoretical similarity analysis. Such analysis provides twofold advantages: it furnishes better understanding of the fundamental phenomena involved, and it saves enormous time and expense in the development of the propulsion system.

The main objective of the similarity analysis is that, by identifying the appropriate similarity rules of the dominant controlling processes, one can define the conditions under which a laboratory-scale "model" system should be tested in order to simulate the behavior of a full-scale (or "prototype") system. Absolute similarity between different-size combustors implies that the different processes occurring in two different-scale systems are of similar fashion, namely, the values of the operating variables such as temperature, pressure, velocity, or concentrations in one system should be linearly related to those at the corresponding points of the other system. As was stated

by Spalding [7], who successfully conducted similarity and model studies in the field of combustion, a complete combustion modeling, which will replicate the similarity rules of every process and effect in different-size combustors, is practically impossible. Hence, in combustion modeling, a partial similarity approach is taken that will preserve the rules of the most significant phenomena and effects, and provide reliable indication of main trends. Such an analysis uses relatively simple concepts and concentrates on the dominant aspects, rather than detailed mathematical modeling. Each individual process is examined in order to assess its relative significance and to find out what should be the operating conditions that would preserve similarity of that process in a different-scale system. Thus, one determines the common conditions which will satisfy the similarity rules of the most important individual processes, and hence the best practical approximation of the overall similarity of the system. Detailed discussion on similarity and scaling in chemically reacting systems is presented by Rosner [8] in his book. A number of similarity studies have been conducted in the field of airbreathing propulsion: Stewart [9,10] investigated the gas turbine combustor, Hottel et al. [11] studied the liquid-fuel ramjet combustor, while Ben-Arosh and Gany [12] applied a comprehensive theoretical and experimental study to the solid fuel ramjet combustor. Gany [13] proposed a theoretical similarity model for the scaling of hybrid motors. No test data were available from direct experimental studies of motors under similarity conditions. Hence, validation of the prediction based on such theoretical similarity analysis has to be accomplished by conducting tests and obtaining appropriate results on motors that are scaled as per the similarity analysis and tested according to similarity conditions.

The objectives of the present investigation are: (1) by taking account of most significant phenomena and effects, to conduct a comprehensive analysis which will specify the most significant similarity conditions in hybrid rocket motors for scaling purposes and predict the scale-effects resulting from such scaling under theoretical similarity conditions, and (2) to validate the derived scaling rules by conducting tests on different-size hybrid rocket motors that are scaled as per similarity requirements and tested under similarity conditions.

It is very important to note, that the idea is not to replace experiments by an absolute theory, but to correctly extend, interpret and use available test data to untested systems of a different size range.

2. Analysis

2.1. Geometry

In general, an obvious similarity requirement in hybrid motors is the geometric similarity, because it directly affects the general flow field pattern in the motor. Maintaining geometric similarity preserves a constant dimension ratio in the major flow zones of different-size combustor. If the fuel grain port diameter d_p is used to represent the scale, then

$$L \propto d_p, \tag{1}$$

where L is the fuel grain length. One may use a single-port laboratory motor to simulate a multiple-port full-scale motor.

2.2. Transport phenomena

Transport phenomena are of major significance in the overall flow and combustion process in hybrid rocket motors. They affect the general flow pattern, boundary layer over the fuel-surface, heat transfer to the surface, diffusion as well as mixing between the fuel and the oxidizer, and the flame characteristics. Hybrid motors are characterized by a turbulent internal flow with dominant boundary layer effects. Hence, the most significant parameter that dominates the flow and transport phenomena is Reynolds number, Re. Similarity of these features can be achieved by requiring the same Reynolds number at the corresponding cross-sections of the related motors:

$$Re = \frac{\rho u d_p}{\mu}. \tag{2}$$

2.3. Mixing process

Similarity of mixing between fuel and oxidizer generally requires constancy of the ratio between the typical mixing rate and the total mass flow rate. Similarity of turbulent mixing can be achieved by constant Reynolds number, Re, whereas molecular mixing has

a minor effect. In general, with the typical turbulent boundary layer nature of the flow in hybrid motors, constancy of Reynolds number ensures similarity of the general flow pattern, including large-scale eddies, fine-scale turbulence, concentration profiles, and other factors and processes such as flame-sheet location, etc.

2.4. Heat transfer

Similarity of heating regimes requires constant ratio between heat transfer to the wall and the overall heat generation (i.e., the rate of heat addition to the flow). With the turbulent nature of the flow, heat transfer in hybrid combustors is mainly attributed to turbulent convection with minor contribution of radiation. Heat transfer to the wall is relative to the heat transfer coefficient h and the temperature difference between the flame and the wall. The overall heat addition rate to the flow is proportional to the mass flow rate times the average temperature increase of the combustion gases. Under geometric similarity both the wall surface area and the port cross-section are proportional to d_p^2. Hence, one obtains

$$h(T_f - T_w)d_p^2 \propto \rho u d_p^2 c_p (T_c - T_i), \tag{3}$$

where T_f, T_w, T_c, and T_i represent the flame, wall, final average and initial temperatures, respectively. Assuming the ratio

$$\frac{T_f - T_w}{T_c - T_i} = \text{const} \tag{4}$$

(resulting from the similarity of the temperature distribution) one can show, by substituting the relevant nondimensional numbers in Eq. (3), that similarity requirement can be expressed by

$$\frac{Nu}{RePr} = \text{const}, \tag{5}$$

where Prandtl number $Pr = \mu c_p/\lambda$ represents a combination of physical properties, and Nusselt number is $Nu = hd_p/\lambda$. In the characteristics combustor regime $Nu = f(Re, Pr)$ and can typically be represented by Reynolds analogy for smooth tubes:

$$Nu = 0.023 Re^{0.8} Pr^{0.33}. \tag{6}$$

Therefore, if a similarity of temperature field is maintained, which also implies similar physical properties in corresponding points in the flow field, then Eq. (3) implies constancy of Nusselt number in addition to Reynolds and Prandtl numbers.

It is noteworthy that the diffusion flame nature of the combustion process in hybrid motors enhances the significance of constancy of Reynolds number in corresponding sections as a result of the domination of physical processes and properties versus chemical aspects.

2.5. Chemical kinetics

Similarity of chemical kinetics requires similarity of temperature and species concentration fields. An obvious need would be the use of the same fuel and oxidizer combination and the same oxidizer/fuel (O/F) ratio. Some specific aspects may yield additional requirements. Characteristic chemical time (i.e. typical combustion time) of hydrocarbon fuels is known to be inversely proportional to pressure, $\tau_{ch} \propto 1/p$. A similar trend is exhibited by the ignition delay time, τ_{ig}. On the other hand, residence time in the combustor can be approximated by $\tau_{res} \propto d_p/u$. Thus constancy of the ratio τ_{ch}/τ_{res} leads to

$$u/(pd_p) = \text{const}. \tag{7}$$

Satisfying Eq. (7) along with a constant Reynolds number, would yield

$$pd_p = \text{const}., \tag{8}$$

as well as a similar velocity field.

It is remarkable to note here that the so-called "pd scaling" (expressed by Eq. (8)), which is one of the most useful scaling techniques for airbreathing combustors [9–11] and which has recently been proven to yield good results for solid fuel ramjet (SFRJ) combustors [12], is also applicable to hybrid rocket motors. However, in spite of the similarities between SFRJ and hybrid motors, one should carefully evaluate its real significance and relevancy to hybrid propulsion.

2.6. Compressibility

Compressibility effects are characterized by Mach number, $M = u/a$, and maintaining similarity of compressibility effects is expressed by constancy of Mach number in corresponding points. With $M = u/\sqrt{\gamma RT}$, such requirement would be fulfilled for simultaneous existence of similar velocity and temperature fields.

3. Model discussion

From the above analysis it is inferred that in hybrid motor the best fulfillment of similarity requirements would be obtained for the following conditions:

(1) geometric similarity,
(2) same oxidizer and fuel combination,
(3) same Reynolds number at corresponding sections,
(4) same value of pd_p in the model and prototype.

In order to consider whether any of these similarity requirements can be relaxed under certain situations, each of these requirements are further examined individually and thus, in the process, the relative significance of each condition is pointed out.

(1) In general, the geometric similarity requirement must be kept; otherwise the system will not be really similar. It is obvious that the motor port diameter increases during the operation, causing some deviation from the initial geometric proportions as well as from the scaling factor. Nevertheless, it is believed that the sensitivity of fuel regression rate predictions to small deviations in this parameter may be within satisfactory limits. On the contrary, the O/F ratio is quite sensitive to the L/d_p ratio and therefore a significant change in L/d_p ratio would certainly affect the overall O/F ratio.

(2) Same fuel and oxidizer combination is mandatory, as it would be very difficult to interpret test results of different combinations.

(3) Considering the fact that in hybrid rockets the physical processes rather than chemical aspects are dominant (e.g. diffusion flame characteristics, turbulent transport phenomena, fuel-oxidizer mixing, etc.), Reynolds number is the single most significant similarity operating parameter. Constancy of Reynolds number in systems under similarity conditions implies

$$Gd_p = \text{const.}, \tag{9}$$

or

$$\frac{\dot{m}}{d_p} = \text{const.} \tag{10}$$

Since

$$\dot{m} = \dot{m}_{ox}\left(\frac{1 + O/F}{O/F}\right) \tag{11}$$

and O/F is expected to be constant under similarity conditions, one obtains the following:

$$G_{ox}d_p = \text{const.} \tag{12}$$

or thus

$$\frac{\dot{m}_{ox}}{d_p} = \text{const.} \tag{13}$$

(4) Constancy of pd_p is a very convincing requirement, which has been found to be one of the major similarity conditions in airbreathing combustors. Its main implication is in keeping similarity of chemistry aspects in the gas phase reactions (in addition to similarity of Mach number). In general, pd_p scaling is supposed to result in the same combustion efficiency. However, since physical rather that chemical aspects dominate the hybrid combustion processes, this requirement may be relaxed, provided that (a) requirement number (3), i.e., the same Reynolds number, is fulfilled; (b) the pressure is sufficiently high, so that chemical kinetics are much faster that physical transport (e.g., diffusion); and (c) an aft-mixing-chamber is used, which would take care of completing the gas phase chemical reactions.

Thus one arrives at the minimum and most significant operating conditions, which would maintain the most dominant similarity parameters and should be kept constant when scaling the hybrid rocket motors. These conditions are:

(1) Geometric similarity, mainly $L \propto d_p$, (in other terms, the ratio of fuel grain length to port diameter should remain constant).
(2) Same fuel and oxidizer combination.
(3) $\dot{m}_{ox}/d_p = \text{const}$ or $Gd_p = \text{const}$ (namely, oxidizer flow rate should be proportional to the motor port diameter).

It is to be noted that in establishing these minimum requirements, it is assumed that in typical operating ranges, pressure effects are minor, and that high combustion efficiency can be maintained by separate means (e.g., orifice diaphragm or aft-mixing chamber). These rules will ensure similarity of the major phenomena and processes and will preserve equality of O/F ratio, Prandtl and Mach numbers in different-size hybrid rocket motors.

One should also note that this analysis does not account for a liquid phase behavior, which may be relevant when a liquid (rather than gaseous) oxidizer is applied. Elaboration on liquid phase aspects was done by Gany [13]. However, as was stated in Ref. [13], when properly designed, the residence time of

the flow in the hybrid motor should be sufficiently long compared to the vaporization time. Hence, in such cases, no specific account should be taken of the liquid phase dynamics in the practical scaling rules.

4. Theoretical performance prediction resulting from the model

Maintaining the above-mentioned operating conditions, the theoretical performance characteristics of the hybrid rocket motor would be as described herein. Testing these results experimentally will validate the similarity model.

4.1. Fuel regression rate

Regression rate of the fuel, which is one of the most significant internal ballistics parameter of hybrid rockets, is generally assumed to be dominated by convective heat transfer to the wall $\dot{q}_w$ and by the heat of gasification or vaporization L_v of the solid fuel (taking into account the sensible heat in addition to the gasification process) according to

$$\dot{r} = \dot{q}_w/(\rho_s L_v) \tag{14}$$

with

$$\dot{q}_w = h(T_f - T_w), \tag{15}$$

where T_f and T_w are flame and wall temperatures, respectively. Substituting the heat transfer coefficient h from the definition of Nusselt number Nu, and using Eq. (6) with a general exponent n of Reynolds number, one can show that, with equality of temperature field and Nusselt number, the resulting regression rate expression is

$$\dot{r} \propto G^n d_p^{n-1}. \tag{16}$$

Since Gd_p is held constant in the similarity model, then, when operating under similarity conditions, one does not have to assume the most appropriate value of n, nor does he have to have information on possible variation along the grain or whether or not the boundary layer is fully developed. The result is expected to be

$$\dot{r} d_p = \text{const.} \tag{17}$$

Namely, under similarity conditions the fuel regression rate is expected to be inversely proportional to the combustor port diameter. In the literature [2–6,14,15], it has been pointed out that at low pressures, regression rate exhibits some pressure dependence. However, at regular operating pressures typical in the hybrid rockets, most investigators have not noticed significant pressure effects, and Eq. (17) is expected to hold still valid.

4.2. Oxidizer/fuel ratio

The fuel flow rate in a hybrid motor is given by

$$\dot{m}_f = \rho_s \dot{r} A_b. \tag{18}$$

As $\dot{r} \propto d_p^{-1}$, Eq. (17), and $A_b \propto d_p^2$ (resulting from the linear proportion of the fuel grain length with the port diameter d_p), one obtains

$$\dot{m}_f \propto d_p. \tag{19}$$

Defining the oxidizer/fuel ratio

$$O/F = \dot{m}_{ox}/\dot{m}_f \tag{20}$$

and combining the similarity requirement, $\dot{m}_{ox}/d_p =$ const., with Eq. (20), indicate that O/F is expected to remain constant under similarity conditions.

4.3. Motor thrust and specific impulse

Motor thrust, F, is given by

$$F = \dot{m} u_e + (p_e - p_a) A_e = C_F c^* \dot{m}. \tag{21}$$

In geometrically similar hybrid motors employing same oxidizer and fuel and with equal O/F and ambient conditions, u_e and p_a are equal in both model and the prototype. In general, the first right-hand side (RHS) term of the above equation dominates the thrust. Since

$$\dot{m} = \dot{m}_{ox} + \dot{m}_f = \dot{m}_{ox}(1 + O/F)/(O/F) \tag{22}$$

and as O/F is expected to be constant, and $\dot{m}_{ox}$ is assumed to be scaled in proportion to d_p, approximately linear proportion between the thrust and motor diameter is expected

$$F \tilde{\propto} d_p. \tag{23}$$

While the product $p_e A_e$ in the second RHS term of Eq. (21) is also proportional to d_p, supporting Eq. (23), the other product $p_a A_e$ is proportional to d_p^2. One may get some deviation from the linearity of

Eq. (23), yielding somewhat lower thrust values than predicted by Eq. (23) at increasing motor sizes.

As far as the theoretical specific impulse is concerned, it can be expressed by

$$I_{sp} = \frac{C_F c^*}{g}. \tag{24}$$

For equal O/F, the theoretical characteristic velocity does not change, i.e., $c^* = \text{constant}$. Thus, I_{sp} is supposed to stay approximately the same

$$I_{sp} \cong \text{const.}, \tag{25}$$

except for somewhat decreasing values for larger motors due to slight variation in C_F resulting from variation in operating pressure.

4.4. Combustion efficiency

If one preserves the similarity in both chemical and mixing aspect, the combustion efficiency is expected to be constant, while motor has to be scaled according to the pd_p scaling rule. However, it is believed that this rigorous requirement may be relieved if good combustion efficiency can be maintained by separate means that are independent of scaling method. Particularly it is known that the use of an orifice plate and a large enough aft-mixing-chamber can ensure satisfactory combustion efficiency.

4.5. Burning time

As pointed out earlier, the fuel regression during the burning process causes continuously increasing deviation from the initial geometric proportions of the hybrid motor. Hence, the systems, which maintain similarity conditions during the initial phase of motor operation, may violate the scaling rules during the overall process. This problem cannot be avoided due to the intrinsic behavior of the hybrid motor, but can be minimized by either conducting short tests or by scaling the motor operation time appropriately. As $\dot{r}$ is proportional to d_p^{-1} and

$$d_p = d_{pi} + 2\dot{r}t_b, \tag{26}$$

the test duration, t_b is scaled according to

$$t_b \propto d_p^2. \tag{27}$$

Namely, the test duration should vary as square of the respective port diameter, and this has to be adequately taken into account when testing hybrid motors. Note that Eq. (27) also indicates the overall burning time of different hybrid systems under similarity conditions.

5. Experimental

A line sketch of the test facility with the motor and its associated control units is illustrated in Fig. 2. In order to permit use of different size motors, the test facility is built as a modular unit. Polymethylmethacrylate (PMMA, Plexiglas®) is used as fuel-grain, and gaseous oxygen (GOX) is used as an oxidizer in all the motors. The fuel grain is placed between the oxygen flow-injector and the upstream end of the aft-mixing-chamber. The other end of the aft-mixing-chamber holds the nozzle assembly. The ignition of the motor is achieved by injecting a small amount of ethylene in the oxygen flow injector for about 300 ms and igniting the resulting oxygen-ethylene mixture using a spark plug. The whole setup is mounted firmly on a flexible thrust stand. During the tests, the oxygen and ethylene flow rates (measured by choked nozzle upstream pressures and temperatures in the oxygen and ethylene supply lines), motor and aft-mixing-chamber pressures, and the thrust are continuously recorded.

Motors having initial port diameters of 7.5, 10, 15, 23, 34, and 40 mm (i.e., five-fold diameter ratio, approximately) and initial geometric proportions, length-to-port diameter ratio, $L/d_p = 10$, were tested. The chamber pressure was always higher than 25 bar in all the tests.

The overall fuel regression rate is calculated from the overall mass loss and the burn time. In general, average values of the different parameters recorded during the motor operation, including the motor port diameter, are used to represent the experimental results. Motor test duration was scaled as per motor initial port diameter and kept constant at a maximum value of 16 s for motors of initial port diameter higher than or equal to 34 mm. This was a compromise between the desire for the same relative final port diameter, which requires burn time in proportion to d_p^2, and the negative aspects resulting from too long burn times and relatively large variations from initial dimensions and proportions.

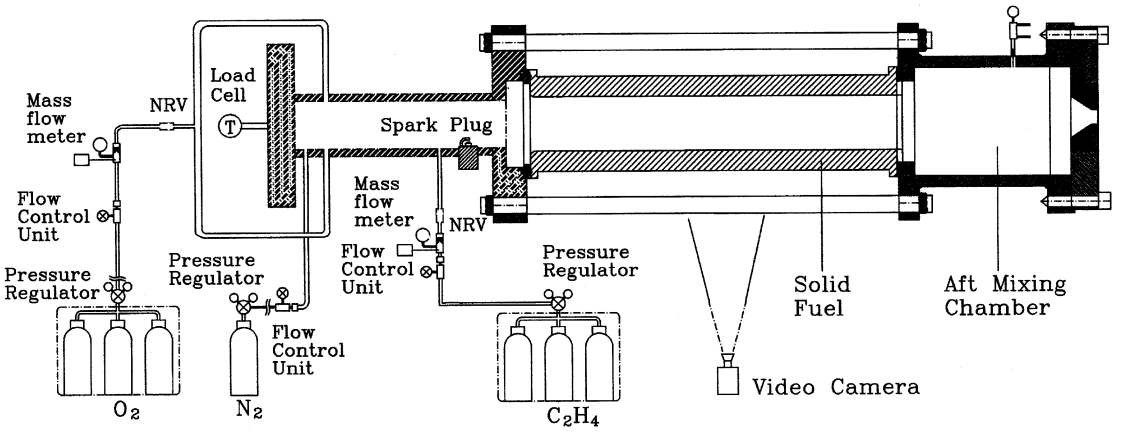

Fig. 2. Hybrid rocket test setup.

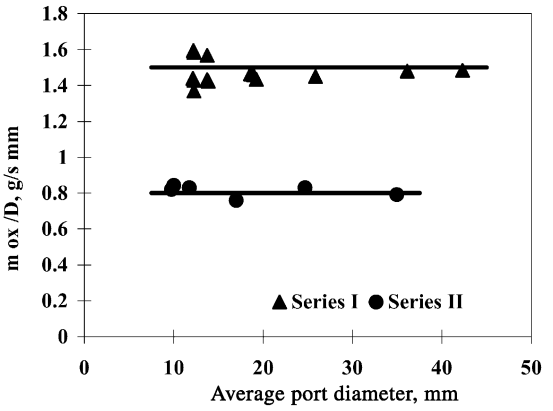

Fig. 3. Actual test conditions showing approximately constant $\dot{m}_{ox}/d_p$ over the range of port diameters for each of the two test series.

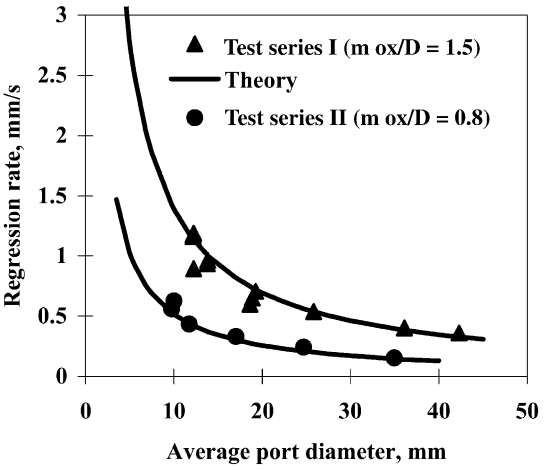

Fig. 4. Regression rate variation with combustor port diameter in Series I & II.

6. Results and discussion

Two test series, namely, Series I at approximately constant value of $\dot{m}_{ox}/d_p = 1.5\ (\pm 10\%)\ g/s$ mm, and Series II at $\dot{m}_{ox}/d_p = 0.8\ (\pm 10\%)\ g/s$ mm, were carried out, as shown in Fig. 3. Fig. 4 represents the theoretical and experimental variations of the regression rate with motor port diameter. The test results agree very well with the theoretical prediction of $\dot{r} \propto d_p^{-1}$, [Eq. (17)], validating the similarity model. In Fig. 5, experimental results of overall oxidizer/fuel (O/F) ratio vs. motor port diameter are shown for the two test series. The stoichiometric O/F ratio for GOX/PMMA system is 1.92. One can see that in all the cases the motor operates at O/F values higher than the stoichiometric value. In each of the test series the oxidizer/fuel ratio seems to be fairly constant within the typical experimental spread, particularly for the larger average port diameters (>15 mm). The theoretical model does not only predict this result, but it actually fulfills important similarity conditions. The motors with smaller port diameters (<15 mm) have increased values of O/F ratio than those of larger port diameters (>15 mm). This may be attributed to the relatively large change in L/D ratio from its

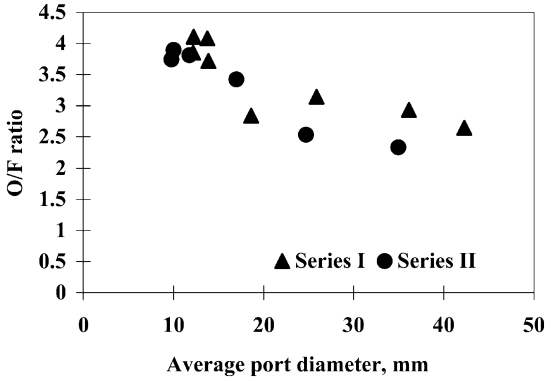

Fig. 5. Experimental results of oxidizer/fuel ratio vs. combustor port diameter.

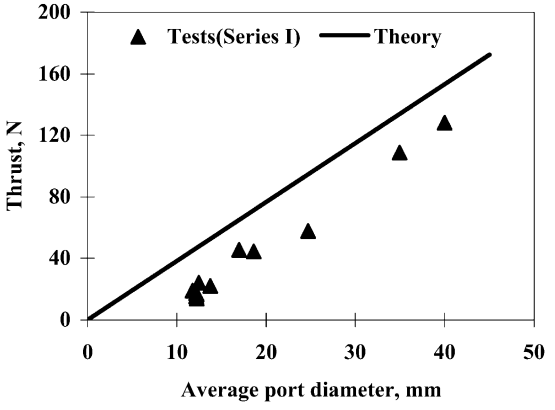

Fig. 6. Motor thrust variation with port diameter for Series I ($\dot{m}_{ox}/d_p = 1.5$).

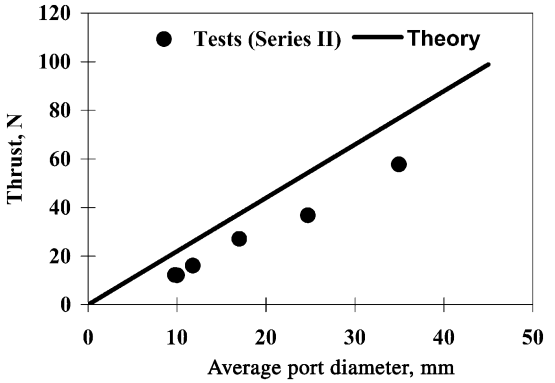

Fig. 7. Motor thrust variation with port diameter for Series II ($\dot{m}_{ox}/d_p = 0.8$).

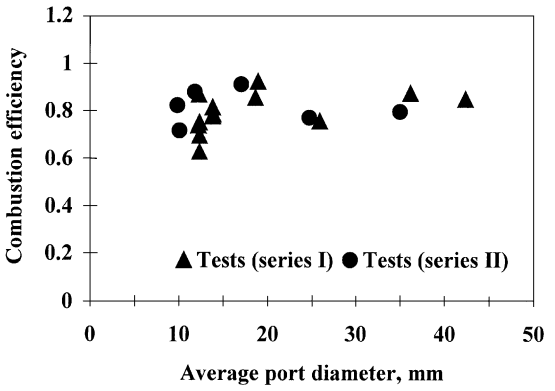

Fig. 8. Variation of combustion efficiency with combustor port diameter.

initial value in smaller port diameter motors, leading to somewhat smaller average L/D ratios and, hence, under-predicted fuel flow rates implying higher O/F ratios in these cases. One can also note, that in the average, the O/F ratio in the second test series (which is of the smaller oxygen flow rate) tends to be somewhat (by about 20%) lower than in the first test series. This behavior agrees with the typical fuel regression rate correlation of approximately $\dot{r} \propto \dot{m}^{0.8}$.

The variation of motor thrust with port diameter is presented in Figs. 6 for Series I and in Fig. 7 for Series II. Both figures show almost linear approximation for the entire range as predicted by Eq. (23). Comparing the experimental values of the thrust with the theoretical values, one can see a similar trend. However, the experimental values are lower because of the lower experimental values of the characteristic velocity, c^*, as indicated by the combustion efficiency data, as well as because of flow losses, lowering the C_F values.

Combustion efficiency, η, is defined in terms of the ratio between the experimental and theoretical [16] values of combustor's characteristic velocity c^*. The test results are summarized in Fig. 8 revealing pretty constant combustion efficiency (typically of the order of 80–90%) for the entire range in both the series. Somewhat lower values of η were obtained in certain tests particularly for the smaller port diameters. These results may be attributed to the higher relative heat losses in the smaller motors.

7. Conclusions

A comprehensive analysis taking account of relevant processes and effects has been carried out in order to define the similarity rules under which laboratory-size hybrid rocket motors should be tested in order to get results that can simulate a full-scale motor. The most significant scaling rules are the following: (1) maintaining geometric similarity, (2) using same oxidizer and fuel combination, (3) scaling $\dot{m}_{ox}$ in proportion to d_p (resulting in $Gd_p = \text{const}$). In order to verify the similarity model and its resulting scaling rules, tests were conducted on laboratory-size PMMA/GOX hybrid rocket motors. The results demonstrated good agreement between the theoretical prediction and the tests of key operating parameters, such as fuel regression rate, O/F ratio, and thrust. Furthermore, the test results not only verify the similarity model and its resulting scaling rules, but also point out that main processes and effects have indeed been adequately taken into account in the theoretical similarity analysis. The overall fundamental result of this study indicates the important role that testing according to the appropriate similarity conditions can play in the development of hybrid motors.

References

[1] G.A. Marxman, G.M. Gilbert, Turbulent boundary layer combustion in hybrid rocket, Proceedings of the Ninth Symposium (International) on Combustion, The Combustion Institute, 1963, pp. 371–383.

[2] C.E. Wooldridge, R.J. Muzzy, Internal ballistic consideration in hybrid rocket design, Journal of Spacecraft and Rockets 4(2) (1967) 255–262.

[3] G.A. Marxman, Boundary layer combustion in propulsion, Proceedings of the 11th Symposium (International) on Combustion, The Combustion Institute, 1967, pp. 269–289.

[4] H.S. Seifert, Hybrid rocket theory and design, in: W.H.T. Loh (Ed.), Jet, Rocket, Nuclear, Ionic and Electric Propulsion: Theory and Design, Springer, New York, 1968, pp. 332–355 (Chapter 7).

[5] T.A. Boardman, Hybrid propellant rockets, in: G.P. Sutton, O. Biblarz (Eds.), Rocket Propulsion Elements, 7th Edition, Wiley, New York, 2001, pp. 579–607 (Chapter 15).

[6] P. Estey, D. Altman, J. McFarlane, An evaluation of scaling effects for hybrid rocket motors, AIAA -91-2517, 27th Joint Propulsion Conference, Sacramento, CA, June 24–26, 1991.

[7] D.B. Spalding, The art of partial modeling, Colloquium on Modeling Principles, Proceedings of the Ninth Symposium (International) on Combustion, The Combustion Institute, 1963, pp. 833–843.

[8] D.E. Rosner, Transport Processes in Chemically Reacting Flow Systems. Dover, Mineola, 2000, pp. 405–454 (Chapter 7).

[9] D.C. Stewart, Scaling of gas turbine combustion systems. AGARD Selected Combustion Problems II, Butterworths Sci. Publications, London, 1956, pp. 384–413.

[10] D.C. Stewart, G.C. Quinns, Similarity and scale effects in ramjet combustors, Proceedings of the Ninth Symposium (International) on Combustion, The Combustion Institute, 1963, pp. 907–922.

[11] H.C. Hottel, G.C. Williams, W.P. Jensen, A.C. Tobey, P.M.R. Burrage, Modeling studies of baffle-type combustors, Proceedings of the Ninth Symposium (International) on Combustion, The Combustion Institute, 1963, pp. 923–935.

[12] R. Ben-Arosh, A. Gany, Similarity and scale effects in solid-fuel ramjet combustors, Journal of Propulsion and Power, AIAA 8(3) (1992) 615–623.

[13] A. Gany, Scale effects in hybrid motors under similarity conditions, AIAA-96-2846, 32nd AIAA/ASME/SAE/ASEE Joint Propulsion Conference, Lake Buena Vista, FL, July 1–3, 1996.

[14] L.E. Smoot, C.F. Price, Pressure dependence of hybrid fuel regression rates, AIAA Journal 5(1) (1967) 102–106.

[15] F.J. Kodson, F.A. Williams, Pressure dependence of non-metallized hybrid fuel regression rates, AIAA Journal 5(4) (1967) 774–778.

[16] D.R. Cruise, Theoretical computations of equilibrium compositions, thermodynamic properties and performance characteristics of propellant systems (PEP Code), NWC-TP-6037, Naval Weapons Center, China Lake, CA, April 1979.